

Near-infrared fluorescent proteins

Dmitry Shcherbo^{1,6}, Irina I Shemiakina^{1,6}, Anastasiya V Ryabova², Kathryn E Luker³, Bradley T Schmidt³, Ekaterina A Souslova¹, Tatiana V Gorodnicheva⁴, Lydia Strukova¹, Konstantin M Shidlovskiy¹, Olga V Britanova¹, Andrey G Zaraisky¹, Konstantin A Lukyanov¹, Victor B Loschenov², Gary D Luker^{3,5} & Dmitriy M Chudakov¹

Fluorescent proteins with emission wavelengths in the near-infrared and infrared range are in high demand for whole-body imaging techniques. Here we report near-infrared dimeric fluorescent proteins eqFP650 and eqFP670. To our knowledge, eqFP650 is the brightest fluorescent protein with emission maximum above 635 nm, and eqFP670 displays the most red-shifted emission maximum and high photostability.

Fluorescent proteins are reliable *in vivo* reporters for whole-body imaging techniques, and the development of far-red light-emitting proteins offered hope that a further red-shift of the emission is possible without dramatic loss of brightness^{1,2}. The next goal was to reach the near-infrared and infrared range, in which living tissues are even more transparent owing to low absorbance and light scattering³. Use of such fluorescent proteins for whole-body imaging would facilitate investigation of metastasis and tumor

localization, cell migration, embryogenesis and other studies involving deep-tissue imaging. Although an infrared protein that requires biliverdin injection for fluorescence has been reported recently⁴, fully genetically encoded markers are preferable. Here we report near-infrared fluorescent proteins based on the dimeric far-red fluorescent protein Katushka².

For whole-body imaging experiments, high reporter expression is usually required, and low cytotoxicity is crucial⁵. According to our experience, Katushka is not cytotoxic, as we have generated stable lines of transgenic *Xenopus laevis*² and *Danio rerio* (Supplementary Fig. 1) expressing Katushka in muscle cells at high levels.

However, a recent report has suggested that more optimal low-toxicity fluorescent protein variants can be selected using a bacterial expression system⁵. We performed a similar screen (Online Methods) and identified a low-cytotoxicity Katushka variant named Katushka-9-5, which had spectral characteristics nearly identical to those of Katushka and had minimal negative impact on bacterial growth, in contrast to Katushka or monomeric

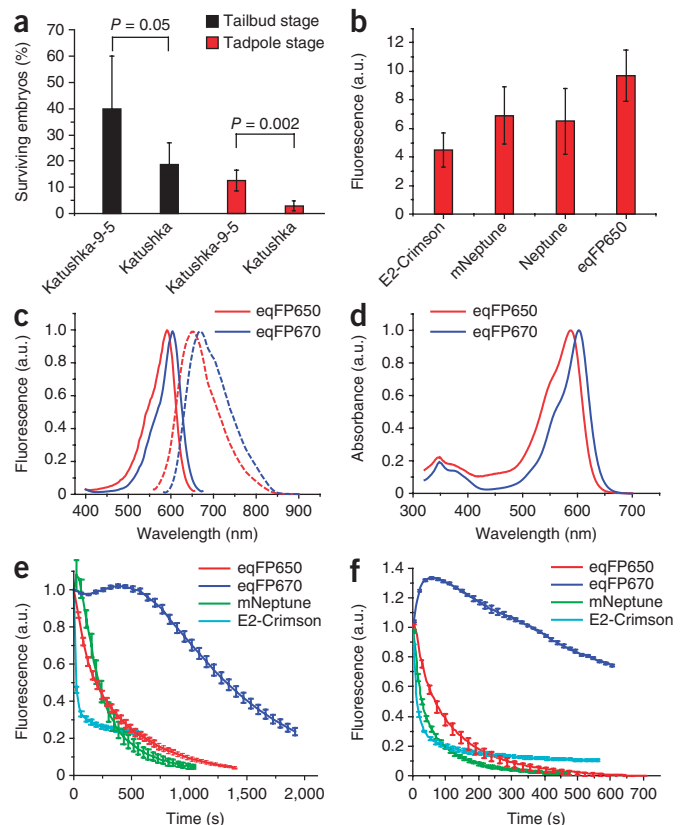


Figure 1 | Cytotoxicity and spectral characteristics. **(a)** Katushka and Katushka-9-5 cytotoxicity in microinjected *X. laevis* embryos. Percentages of surviving embryos by the tailbud and tadpole stages are shown (means \pm s.d.; $n = 5$ experiments each performed on 60 embryos). Significance was analyzed by Student's *t*-test. **(b)** Flow cytometry analysis of HeLa cells 48 h after transient transfection with vectors encoding E2-Crimson, mNeptune, Neptune and eqFP650. Fluorescence brightness was normalized to the relative efficiency of excitation by the 488 nm laser line used. Emission was collected at 660–700 nm. Means \pm s.d. are shown ($n \geq 3$ transfection experiments). **(c)** Normalized fluorescence excitation (solid lines) and emission (dashed lines) spectra for eqFP650 and eqFP670. **(d)** Normalized absorption spectra for eqFP650 and eqFP670. **(e, f)** Normalized photobleaching curves for eqFP650, eqFP670, mNeptune and E2-Crimson using widefield fluorescence microscopy under metal halide illumination **(e)** or laser-scanning confocal microscopy **(f)**. Error bars, s.d. ($n = 4$ experiments).

¹Shemiakin-Ovchinnikov Institute of Bioorganic Chemistry, Russian Academy of Science, Moscow, Russia. ²A.M. Prokhorov General Physics Institute, Russian Academy of Science, Moscow, Russia. ³Center for Molecular Imaging, University of Michigan Medical School, Ann Arbor, Michigan, USA. ⁴Evrogen JSC, Moscow, Russia.

⁵Department of Microbiology and Immunology, University of Michigan Medical School, Ann Arbor, Michigan, USA. ⁶These authors contributed equally to this work. Correspondence should be addressed to D.M.C. (chudakovdm@mail.ru).

Table 1 | Key characteristics of far-red fluorescent proteins

	mCherry	Katushka	RFP639	E2-Crimson	mNeptune	eqFP650	eqFP670
Excitation peak (nm)	587	588	588	605	599	592	605
Emission peak (nm)	610	635	639	646	649	650	670
Fluorescence quantum yield	0.22	0.34	0.18	0.12	0.18	0.24	0.06
Molar extinction coefficient ($M^{-1} \text{ cm}^{-1}$) at excitation maximum	72,000	65,000	69,000	58,500	57,500	65,000	70,000
Brightness ^a (a.u.)	15,840	22,100	12,420	7,080	10,350	15,600	4,200
Molar extinction coefficient ($M^{-1} \text{ cm}^{-1}$) at 635 nm	1,000	1,700	~2,000	12,640	7,900	4,300	15,700
Quantum yield in infrared (700–900 nm)	0.04	0.07	~0.05	0.03	0.05	0.07	0.03
Brightness in infrared ^b (a.u.)	40	119	~100	379	395	301	471
Photostability, widefield ^c (s)	601	ND	ND	19	216	190	1,289
Photostability, confocal ^c (s)	48	77	ND	14	29	67	>700
pKa	4.5	5.5	ND	ND	5.8	5.7	4.5
Reference	9	2	10	8	6	This work	This work

Proteins are ordered according to the position of emission maximum. ND, not determined.

^aCalculated as the product of the molar extinction coefficient and quantum yield. ^bCalculated as the product of the extinction coefficient at 635 nm, quantum yield and emission fraction between 700 nm and 900 nm. ^cTime to bleach 50% of fluorescence signal brightness.

(m)Neptune, a recently reported monomeric far-red fluorescent protein⁶ (Supplementary Fig. 2). Neither Katushka-9-5 nor Katushka demonstrated any visible cytotoxicity when expressed in mammalian HeLa cells (Supplementary Fig. 3). To compare cytotoxicity of Katushka-9-5 and Katushka *in vivo*, we micro-injected plasmids in the animal poles of *X. laevis* embryos at the two-cell stage (20 pg per blastomere), and tracked the death rate by the tailbud stage (stage 25) and by the tadpole stage (stage 42). These experiments demonstrated lower toxicity of Katushka-9-5 compared to Katushka (Fig. 1a).

Because of its lower toxicity, we selected Katushka-9-5 for the development of fluorescent protein variants with further red-shifted emission. Based on the crystal structure of the related far-red fluorescent protein mKate⁷ (Protein Data Bank (PDB): 3BXB), we selected amino acid positions in proximity to the chromophore (including Met14, Leu16, Met44, Thr62, Tyr121, Ser148, Ser165, Met167, Arg203 and Leu205) for targeted mutagenesis (numbering in accordance with *Aequorea victoria* GFP, avGFP; Supplementary Fig. 4). We performed semisaturated (two to five amino acid variants) site-directed mutagenesis of these positions in several combinations and random mutagenesis. We manually screened bacterial libraries containing these mutants using a fluorescence stereomicroscope equipped with a 650LP emission filter and a built-in spectrofluorimeter. We screened more than a million individual colonies and selected two red-shifted variants, named *Entacmaea quadricolor* (eq)FP650

and eqFP670, that had substitutions N24G,M44A and M14T,N24G,M44C,S148N,S165N, respectively. Notably, Met44 is also substituted by a small amino acid in two recently published far-red fluorescent proteins, mNeptune⁶ and E2-Crimson⁸ (Supplementary Fig. 4). This mutation has been shown to create a cavity filled by a water molecule forming a hydrogen bond with the chromophore acylimine oxygen⁶ and appears to be a universal solution for providing a bathochromic shift of the fluorescence emission for DsRed-like chromophores.

Characteristics of eqFP650 and eqFP670 are summarized in Table 1 and Figure 1. Both proteins were characterized by fast maturation in *Escherichia coli* at 37 °C and demonstrated no residual short-wavelength fluorescence of intermediate or alternative chromophore forms, in contrast to E2-Crimson, which exhibits a second bright blue emission peak, and mNeptune, which has a pronounced green peak (Supplementary Fig. 5). As evidence of complete chromophore maturation, the

absorbance spectra of freshly purified proteins were single peaks with minor absorption bands at 340–360 nm characteristic of red fluorescent proteins (Fig. 1d). In transiently transfected HeLa cells, eqFP650 produced the brightest signal in its spectral class (Fig. 1b). In HEK-293T cells that provide high expression, eqFP650 produced bright signal 14 h after transfection.

eqFP650 and eqFP670 had only one amino-acid substitution in the outer surface of the beta-barrel (Gly24, characteristic for avGFP and E2-Crimson, Supplementary Fig. 4) and both inherited the dimeric nature of Katushka-9-5, as well as its low toxicity in bacterial expression experiments (Supplementary Fig. 2). In eukaryotic cells, eqFP650 and eqFP670 were evenly distributed and demonstrated no aggregation or toxicity (Supplementary Fig. 6).

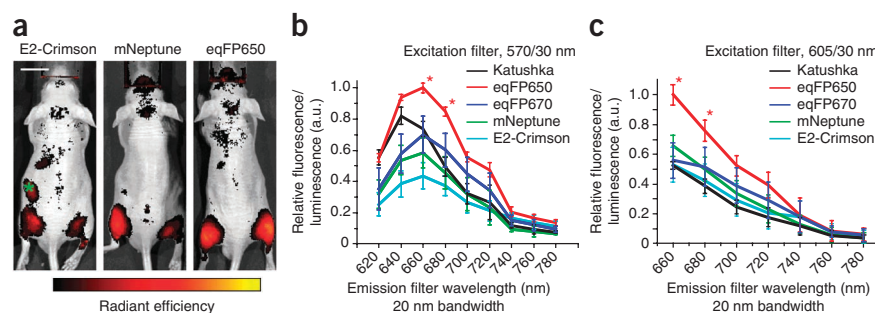


Figure 2 | Whole-mouse imaging with IVIS Spectrum system (Caliper). (a) Representative fluorescence reflectance images (excitation filter, 605/30 nm and emission filter, 660/20 nm) of mice injected intramuscularly with HEK 293T cells expressing E2-Crimson, mNeptune or eqFP650. Asterisk denotes background fluorescence in mice injected with E2-Crimson cells. Scale bar, 1 cm. The color bar indicates radiant efficiency $\times 10^{-6}$; minimum is 0.001, and maximum is 0.006. (b,c) Fluorescence efficiency from cell implants imaged with 570/30 nm (b) or 605/30 nm (c) excitation filters and various emission filters, normalized to photons from firefly luciferase to control for transfection efficiency and numbers of implanted cells. Means \pm s.e.m. are shown ($n = 6-10$ per point). * $P < 0.05$ (Student's *t*-test) for eqFP650 relative to other proteins.

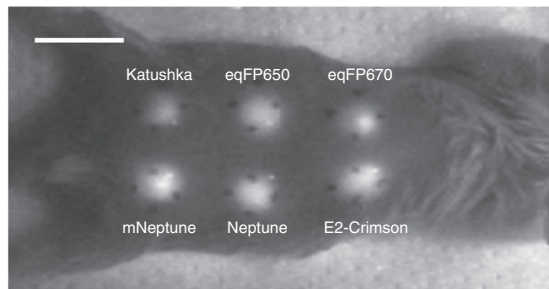


Figure 3 | Whole-mouse infrared imaging with the Biospec system. Infrared fluorescence of subcutaneous injections of equal amounts of protein samples into a living mouse after normalization using the extinction coefficient at the absorption maximum wavelength of each protein. Excitation at 635 nm with photodiodes was used, and emission was measured over the integrated 700–900 nm range. Scale bar, 1 cm.

eqFP650 generally retained the high brightness of Katushka and was characterized by a strong bathochromic shift, with excitation and emission peaks at 592 nm and 650 nm, respectively (Fig. 1c and Supplementary Fig. 7). To date, eqFP650 is the brightest fluorescent protein with emission maxima above 635 nm and should be an optimal genetically encoded marker for *in vivo* imaging.

eqFP670 is characterized by lower brightness but stronger bathochromic shift, with excitation and emission peaks at 605 nm and 670 nm. eqFP670 is to our knowledge the first GFP-like fluorescent protein with such long-wavelength emission, approximately half of which falls in the infrared part of the spectrum. Compared to Katushka, eqFP670 had fourfold greater infrared brightness (Table 1). Furthermore, eqFP670 had high pH stability (Table 1) and extremely high photostability (Fig. 1e,f) and should allow for accumulation of the fluorescent signal over long exposure times. The combination of Asn148 and Asn165 in eqFP670 is unique and has not been encountered in other fluorescent proteins. This implies tight packing around the chromophore, which probably forms the basis of the high photostability and pH resistance.

To investigate fluorescence detection in deep tissues by whole-animal imaging, we transiently transfected HEK 293T cells with a plasmids encoding either Katushka, eqFP650, eqFP670, mNeptune⁶ or E2-Crimson⁸ and injected cells intramuscularly into the gluteal region of mice. We also transfected these cells with firefly luciferase plasmid to normalize for transfection efficiency and total numbers of injected cells. Representative images of mice injected with cells expressing E2-Crimson, mNeptune or eqFP650 showed that eqFP650 had the highest fluorescence (Fig. 2a), and quantification at various emission wavelengths showed higher fluorescence from eqFP650 at two excitation wavelengths (Fig. 2b,c). No cell implant was detectable with 640 nm excitation and infrared detection, probably owing to the high background signal.

To compare efficiency of infrared imaging, we used another imaging system. We subcutaneously (2-mm depth) injected equal portions of mature Katushka, eqFP650, eqFP670, E2-Crimson, Neptune and mNeptune protein. Injection of protein samples

provided higher local concentration of a fluorescent protein than injection of transiently transfected cells, allowing for better signal-to-noise ratio. In this artificial system, all the proteins tested had comparable infrared signal (Fig. 3). This system, however, did not account for multiple influences on fluorescent protein signal in living cells that were present in the *in vivo* experiment shown in Figure 2, such as protein maturation rate, protein turnover, mRNA stability and transcription rate. We did not attempt to quantify protein expression and do not know how it may have varied.

Although we demonstrated that eqFP650 now may be the preferable near-infrared fluorescent protein for *in vivo* cell-labeling experiments, we believe that development of longer-wavelength fluorescent proteins such as eqFP670 with high brightness and of true monomeric variants for protein fusions will increase the sensitivity and capabilities of deep-tissue imaging techniques.

METHODS

Methods and any associated references are available in the online version of the paper at <http://www.nature.com/naturemethods/>.

Accession codes. GenBank: HQ148301 (eqFP650) and HQ148302 (eqFP670).

Note: Supplementary information is available on the Nature Methods website.

ACKNOWLEDGMENTS

We thank J.M. Steele for technical assistance with mouse experiments and B.S. Glick (University of Chicago) for providing the plasmid encoding E2-Crimson. This work was supported by grants from the Molecular and Cell Biology program of the Russian Academy of Sciences, the Howard Hughes Medical Institute (55005618), the US National Institutes of Health (R01CA136553, R01CA136829 and P50CA093990), Rosnauka (02.512.12.2053) and the Russian Foundation for Basic Research (08-04-01702-à and 10-04-01042).

AUTHOR CONTRIBUTIONS

D.S., I.I.S. and L.S. developed fluorescent proteins. A.V.R. and V.B.L. performed experiments on a Biospec imaging system. K.E.L., B.T.S. and G.D.L. performed experiments on a Caliper IVIS spectrum imaging system. A.G.Z. performed experiments on *Xenopus* embryos. T.V.G. and E.A.S. grew cells and performed microscopy experiments. K.M.S. generated transgenic zebrafish. O.V.B. performed flow cytometry analysis. K.A.L., G.D.L. and D.M.C. designed and planned the project and wrote the manuscript.

COMPETING FINANCIAL INTERESTS

The authors declare competing financial interests: details accompany the full-text HTML version of the paper at <http://www.nature.com/naturemethods/>.

Published online at <http://www.nature.com/naturemethods/>.

Reprints and permissions information is available online at <http://npg.nature.com/reprintsandpermissions/>.

- Hoffman, R.M. *J. Biomed. Opt.* **10**, 41202 (2005).
- Shcherbo, D. *et al. Nat. Methods* **4**, 741–746 (2007).
- Deliolanis, N.C. *et al. J. Biomed. Opt.* **13**, 044008 (2008).
- Shu, X. *et al. Science* **324**, 804–807 (2009).
- Strack, R.L. *et al. Nat. Methods* **5**, 955–957 (2008).
- Lin, M.Z. *et al. Chem. Biol.* **16**, 1169–1179 (2009).
- Pletnev, S. *et al. J. Biol. Chem.* **283**, 28980–28987 (2008).
- Strack, R.L. *et al. Biochemistry* **48**, 8279–8281 (2009).
- Shaner, N.C. *et al. Nat. Biotechnol.* **22**, 1567–1572 (2004).
- Kredel, S. *et al. Chem. Biol.* **15**, 224–233 (2008).

ONLINE METHODS

Cloning and gene construction. Cloning and gene construction were performed as described in reference 2. Briefly, purification of PCR products and products of restriction digests was performed by gel electrophoresis and extraction using the QIAquick gel extraction kit (Qiagen). Plasmid DNA was purified using the QIAprep Spin Miniprep kit (Qiagen). Site-directed mutagenesis was performed by overlap-extension PCR¹¹. Random mutagenesis was performed using the Diversity PCR Random Mutagenesis kit (Clontech). For bacterial expression, a fluorescent protein gene was cloned into the pQE30 vector (Qiagen) using BamHI and HindIII restriction sites. For expression in eukaryotic cells, a fluorescent protein gene was cloned instead of *TurboGFP* into the pTurboGFP-N vector (Evrogen) using AgeI and NotI restriction sites.

Characterization of fluorescent proteins *in vitro*. Fluorescent proteins were characterized as described in reference 12. Briefly, proteins were expressed in *E. coli* XL1 Blue strain (Invitrogen), purified using Talon metal-affinity resin (Clontech) and desalted using gel-filtration columns (Bio-Rad). Cary 100 UV/VIS Spectrophotometer and Varian Cary Eclipse Fluorescence spectrophotometer were used to measure absorption and excitation-emission spectra. All measurements were performed in 100 mM NaCl with 20 mM Tris-HCl (pH 7.5). Molar extinction coefficients were calculated based on the chromophore absorption in native proteins and proteins alkali-denatured with an equal volume of 2 M NaOH, considering that in alkaline conditions DsRed-like chromophore converts to the GFP-like one¹³ with an extinction coefficient of 44,000 M⁻¹ cm⁻¹ at 452 nm. Absorbance spectra were measured immediately after denaturation. Quantum yields were determined by direct comparison with mCherry. To measure pH stability, buffers in the pH range from 3 to 10 were used. An aliquot of purified protein was diluted in the corresponding buffer solution. After 1 h incubation at room temperature (25 °C), the fluorescence brightness was measured. In each sample, actual final pH was measured using a microelectrode (Sartorius).

Photostability. Selected proteins underwent a photostability comparison test in LSM 510 confocal scanning microscope (Carl Zeiss) and epifluorescence Leica AFLX 6000 microscope. Proteins with 6His tags were bound to Talon metal affinity resin beads, placed on a glass slide and exposed to light. The following

parameters were used for bleaching by a 561 nm laser line in a confocal microscope: 63× oil-immersion objective, 1.5× zoom, 4 s per image scan rate and maximal power. For bleaching by a mercury arc lamp, a TexasRed filter set was used, which passes the 546 nm peak of a mercury lamp. Bleaching times were corrected on the molar extinction coefficients of the corresponding fluorescent protein at 546 nm or 561 nm.

Animal imaging and data analysis. HEK 293T cells were grown in DMEM (Invitrogen), 10% FBS, 1% glutamine and 0.1% penicillin-streptomycin-gentamicin. Cells were transfected with 8.7 µg of plasmid encoding various fluorescent proteins and 1 µg of plasmid encoding firefly luciferase by calcium phosphate precipitation as described previously¹⁴. Cells were used for experiments 2 d after transfection. The plasmid for E2-Crimson was provided courtesy of B. Glick (University of Chicago). All animal procedures were approved by the University of Michigan Committee on Use and Care of Animals. Mice were anesthetized with isoflurane and injected with 2.5 × 10⁶ cells intramuscularly into the right and left gluteal musculature of each mouse. Cells were injected in 100 µl of a 1:1 mixture of F12 medium and matrigel (BD Biosciences). Imaging was performed approximately 1 h after injection. Bioluminescence and fluorescence imaging were performed on an IVIS Spectrum (Caliper) system. Fluorescence images were acquired with excitation and emission filters indicated in **Figure 2**, using 3-s acquisition, small binning and 12.5-cm field of view. After fluorescence imaging, bioluminescence imaging of firefly luciferase was performed as described previously¹⁵. Data for fluorescence and bioluminescence were quantified as efficiency and photons, respectively. To account for differences in transfection efficiency and actual numbers of injected cells, pseudocolor displays for fluorescence images were normalized for photons for firefly luciferase in each cell implant. Data were also graphed as ratios of fluorescence efficiency to firefly luciferase photons and presented as mean values ± s.e.m. (*n* = 4–6 samples per point).

11. Ho, S.N., Hunt, H.D., Horton, R.M., Pullen, J.K. & Pease, L.R. *Gene* **77**, 51–59 (1989).
12. Shcherbo, D. *et al. Biochem. J.* **418**, 567–574 (2009).
13. Gross, L.A., Baird, G.S., Hoffman, R.C., Baldrige, K.K. & Tsien, R.Y. *Proc. Natl. Acad. Sci. USA* **97**, 11990–11995 (2000).
14. Smith, M.C. *et al. Cancer Res.* **64**, 8604–8612 (2004).
15. Luker, G.D. *et al. J. Virol.* **76**, 12149–12161 (2002).